

pubs.acs.org/JACS Article

C-H Amination Mediated by Cobalt Organoazide Adducts and the Corresponding Cobalt Nitrenoid Intermediates

Yunjung Baek, Anuvab Das, Shao-Liang Zheng, Joseph H. Reibenspies, David C. Powers, and Theodore A. Betley*



Cite This: J. Am. Chem. Soc. 2020, 142, 11232-11243



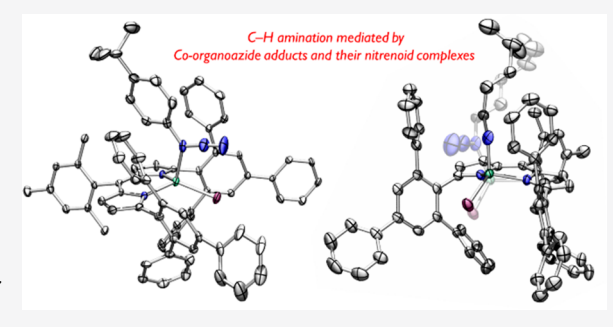
ACCESS

III Metrics & More

Article Recommendations

Supporting Information

ABSTRACT: Treatment of (^{Ar}L)CoBr (^{Ar}L = 5-mesityl-1,9-(2,4,6-Ph₃C₆H₂)dipyrrin) with a stoichiometric amount of 1-azido-4-(^{4r}L)butyl)benzene N₃(C₆H₄- ^{4r}P - 4 Bu) furnished the corresponding four-coordinate organoazide-bound complex (^{Ar}L)CoBr(N₃(C₆H₄- ^{4r}P - 4 Bu)). Spectroscopic and structural characterization of the complex indicated redox innocent ligation of the organoazide. Slow expulsion of dinitrogen (N₂) was observed at room temperature to afford a ligand functionalized product via a [3 + 2] annulation, which can be mediated by a high-valent nitrene intermediate such as a Co^{III} iminyl (^{4r}L)CoBr(^{4r}L)CoBr(^{4r}L)CoBr(N(C₆H₄- ^{4r}P - ^{4r}Bu)) complex. The presence of the proposed intermediate and its viability as a nitrene group transfer



reagent are supported by intermolecular C–H amination and aziridination reactivities. Unlike (^{Ar}L)CoBr(N_3 (C_6H_4 -p- tBu)), a series of alkyl azide-bound Co II analogues expel N_2 only above 60 $^{\circ}C$, affording paramagnetic intermediates that convert to the corresponding Co-imine complexes via α -H-atom abstraction. The corresponding N_2 -released structures were observed via single-crystal-to-crystal transformation, suggesting formation of a Co-nitrenoid intermediate in solid-state. Alternatively, the alkyl azide-bound congeners supported by a more sterically accessible dipyrrinato scaffold ^{tBu}L (^{tBu}L = 5-mesityl-(1,9-di-*tert*-butyl)dipyrrin) facilitate intramolecular 1,3-dipolar cycloaddition as well as C–H amination to furnish 1,2,3-dihydrotriazole and substituted pyrrolidine products, respectively. For the C–H amination, we observe that the temperature required for azide activation varies depending on the presence of weak C–H bonds, suggesting that the alkyl azide adducts serve as viable species for C–H amination when the C–H bonds are (1) proximal to the azide moiety and (2) sufficiently weak to be activated.

1. INTRODUCTION

Transition metal mediated C–H amination is an appealing synthetic route for direct incorporation of N-functionality into unactivated C–H bonds. $^{1-6}$ For such transformations, metal nitrene complexes (e.g., imido, $M(NR^{2-});^{7-9}$ iminyl, M- $(^2NR^-);^{10-19}$ nitrene adducts, $M(^3NR)^{20,21}$) have been invoked as viable N-group transfer reagents, attracting great interest for synthesizing these complexes. 22 Toward this end, N_2 extrusion from organoazides (N_3R) represents one of the most common approaches to generate metal nitrene complexes. 23 As such, while many metal nitrene compounds have been isolated, the corresponding precursors, metal-organoazide adduct complexes are relatively rare due to rapid N_2 expulsion. 24

Despite the transient nature of metal-organoazide adduct complexes, a few examples have been structurally characterized. Owing to the possible resonance structures and the dipolar character of the azide moiety, several binding modes of organoazides toward transition metals have been observed. For example, organoazides bound to an early transition metal such as tantalum, vanadium, van

short $M-N_{\gamma}$ distance due to a π -back bonding interaction. This binding mode is most commonly observed when the organoazide behaves as a dianionic ligand in the form of a diazenimido (Figure 1a). In contrast, organoazides prefer to bind in a neutral (redox-innocent) fashion to late transition metals (e.g., palladium, ²⁴ iridium, ³¹ copper, ³² silver, ³² ruthenium, ³³ and cobalt ³⁴) and exhibit a relatively linear N-N-N moiety (Figure 1b-c). Interestingly, an iron-based organoazide adduct reported by the Peters group manifests intermediate binding properties of the aforementioned two extremes by displaying a partially oxidized iron center along with a bent N-N-N moiety owing to a spin delocalization through the azide moiety (Figure 1d). ³⁵ In addition to these η^1 -type interactions, an η^2 -coordination has been observed by Hillhouse using a 1,2-bis(di-tert-butylphosphino)ethane nickel

Received: April 18, 2020 Published: May 26, 2020





(a)
$$M^{(n+2)} = N_{\gamma} \stackrel{N}{\sim} N^{R}$$
 (b) $M^{n} \leftarrow N_{\gamma} = N = N^{R}$ (c) $M^{n} \leftarrow N_{\alpha} \stackrel{R}{\leftarrow} N_{\alpha} \stackrel{N}{\leftarrow} N_$

Figure 1. Observed binding modes of organoazides to a metal center(s).

complex (Figure 1e).³⁶ Moreover, μ^2 -coordination has been observed with a heterobinuclear complex composed of zirconium and iridium (Figure 1f).³⁷

Each binding mode can dictate a discrete decomposition pathway for conversion to the corresponding metal nitrene compounds. ^{26,27,29,36,37} Moreover, in a few cases, metalorganoazide adducts, and not the corresponding metal nitrene complexes, are proposed as viable nitrene group transfer reagents as elucidated by kinetic analysis. ^{25,38–40} Thus, studying the nature of the binding interaction and the electronic structure of organoazide-bound metal complexes becomes critical for investigating subsequent nitrene group transfer reactions.

Our group has previously demonstrated both intra- and intermolecular C–H amination mediated by Fe^{III} iminyl species generated from dipyrrinato Fe^{II} complexes and various organoazides. $^{11-13,41}$ In the synthesis of these ferric iminyl complexes, the corresponding organoazide-bound iron complexes have been invoked as intermediate species. However, no such intermediate was detected due to extremely fast N_2 extrusion. Similarly, organoazide adducts have been often proposed as relevant precursors in other late, first-row transition metal-catalyzed C–H amination processes, $^{15,42-44}$ yet structural evidence for those species is absent.

In order to unveil the presence and structural identity of transient organoazide-bound metal complexes, we chose to investigate analogous dipyrrinato cobalt complexes as cobalt is typically harder to oxidize given its higher electronegativity relative to iron. With this approach, we report herein the synthesis and spectroscopic characterization of a series of organoazide-bound dipyrrinato Co^{II} complexes. By utilizing a sterically encumbered dipyrrin scaffold ArL (ArL = 5-mesityl-1,9-(2,4,6-Ph₃C₆H₂)dipyrrin), we were able to crystallographically characterize both aryl and alkyl azide-bound Co complexes. From those adduct species, we demonstrate a range of intra- and intermolecular C-H activation processes as well as N-group transfer reactivity, which is proposed to be mediated by a high-valent nitrenoid intermediate such as a Co^{IV} imido or Co^{III} iminyl species. Indeed, using alkyl azide adducts, we were able to directly observe the proposed highvalent Co-nitrene intermediate within a crystal lattice following either thermolysis or X-ray irradiation of single crystals of the azide adducts. Alternatively, a more sterically accessible ligand ^{tBu}L ($^{tBu}L = 5$ -mesityl-(1,9-di-tert-butyl)dipyrrin) offers greater flexibility to analogous alkyl azide adducts enabling facile intramolecular C-H amination to afford substituted pyrrolidines. Detailed mechanistic studies on the C-H amination processes establish the competency of the azide adduct itself to undergo C-H amination without necessitating a high-valent metal nitrenoid intermediate.

2. RESULTS AND DISCUSSION

2.1. Synthesis of Cobalt Organoazide Adducts. Our group has previously reported the preparation of both fourand three-coordinate dipyrrinato Co^{II} complexes, $\binom{Ar}{L}CoCl(py)$ $\binom{Ar}{L} = 5$ -mesityl-1,9-(2,4,6- $Ph_3C_6H_2$)dipyrrin) (1)⁴⁵ and $\binom{Ar}{L}CoBr$ (2),⁴⁶ respectively. We envisioned that treatment of such Co^{II} complexes with an organoazide would furnish either the corresponding organoazide-bound complexes or cobalt nitrene species. Heating a solution of 1 in benzene- d_6 with 1-azido-4-(tert-butyl)benzene $N_3(C_6H_4$ -p-tBu) at 60 °C, however, affords no reaction. In contrast, the coordinatively less saturated complex 2 rapidly consumes the azide at room temperature to generate a new paramagnetic species as verified by tH NMR spectroscopy.

Crystals of this product were obtained from a toluene/pentane mixture at -35 °C. X-ray diffraction analysis revealed formation of the corresponding four-coordinate aryl azide-bound complex (^{Ar}L)CoBr(N_3 (C_6H_4 -p- tBu)) (3) (Scheme 1,

Scheme 1. Synthesis of 3

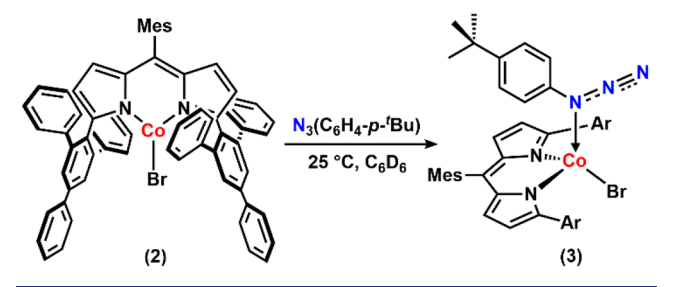


Figure 2). The solid-state structure of 3 exhibits a distorted trigonal monopyramidal geometry ($\tau_4 = 0.80$), ⁴⁷ featuring an axially coordinated aryl azide with a Co–N $_{\alpha}$ distance of 2.111(5) Å, and a nearly linear N $_{\alpha}$ –N $_{\beta}$ –N $_{\gamma}$ angle of 174.8(7) °. Additionally, an intramolecular π – π stacking between the aryl unit of the parent organoazide and one of the phenyl rings

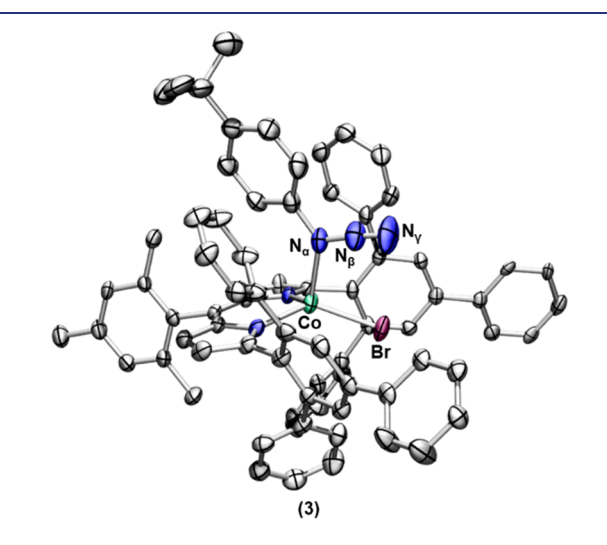


Figure 2. Solid-state structure of **3** at 100 K with thermal ellipsoids set to the 50% probability level (hydrogen atoms and solvent molecules are omitted for clarity; Co aquamarine; C gray; N blue; Br, maroon). Selected bond lengths (Å) and angles (deg) for **3**: Co-N $_{\alpha}$ 2.111(5); N $_{\alpha}$ -N $_{\beta}$ 1.282(7); N $_{\beta}$ -N $_{\gamma}$ 1.125(7); and N $_{\alpha}$ -N $_{\beta}$ -N $_{\gamma}$ 174.8(7).

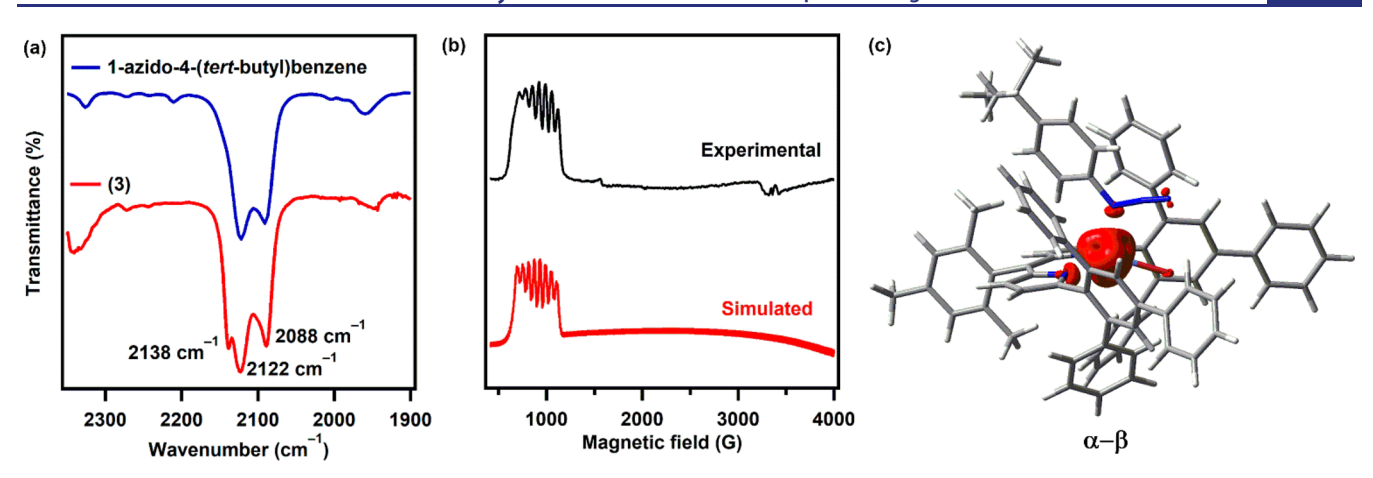


Figure 3. (a) Solution IR spectra of free 1-azido-4-(*tert*-butyl)benzene (above, blue) and 3 (below, red) in benzene. (b) EPR spectrum of 3 in frozen toluene at 4 K (above, black) and its simulation (below, red); simulation parameters: $S = \frac{3}{2}$, $g_1 = 2.4$, $g_2 = 2.4$, $g_3 = 2.4$; $A_{1(Co)} = 0$ MHz, $A_{2(Co)} = 600$ MHz, $A_{3(Co)} = 200$ MHz. (c) Mulliken spin-density plot calculated for 3.

Scheme 2. Intra- and Intermolecular Nitrene Group Transfer Reactivity of 3

from the 2,4,6-triphenylphenyl substituents was observed (Figure S1 of the Supporting Information, SI). 48,49

We note that complex 3 displays a relatively rare binding mode of the organoazide, where the cobalt center coordinates to the N_{α} as opposed to terminal N_{γ} ligation. To date, only a few complexes feature this binding motif, most of which feature a second- or third-row transition metal such as Rh, ⁵¹ Pd, ²⁴ Ag, ³² Ir, ³¹ or Au. ⁵² Among first-row transition metals, a bis(pyrrolyl)pyridine pincer cobalt(II) complex is the only example reported to exhibit a similar interaction with 1-azidoadamantane. ³⁴ We note that neither mono nor bis *ortho*-substituted aryl azides exhibits observable binding to 2, highlighting the preferred Co– N_{α} interaction over the more sterically accessible N_{γ} .

2.2. Electronic Structure of 3. As mentioned above, the binding mode of the organoazide observed for 3 is rare, especially for first-row transition metals. In addition, given that

the steric profile of organoazides is not the dominating factor that dictates the binding mode, we hypothesized that 3 may favor certain electronic configurations. As such, we sought to investigate the electronic structure of 3 by characterizing the binding properties of the organoazide. First, as the bond length of Co-N_{α} (2.111(5) Å) is within the range of a Co-N single bond, we speculated that 3 can be best described as a Lewis acid—base pair. Moreover, we observed that aryl azides such as 2-azido-1,3,5-trifluorobenzene or 1-azido-2,3,4,5,6-pentafluorobenzene display no binding affinity toward 2, suggesting that the relatively electron deficient aryl azides are not sufficiently donating. These results are in line with the lack of reactivity between 1 and 1-azido-4-(*tert*-butyl)benzene as pyridine is more Lewis basic than the aryl azide, suggesting a simple dative interaction between the cobalt and the organoazide.

The solution IR spectrum of 3 in benzene revealed a distinct blue-shifted $\nu(N_3)$ stretch at room temperature, indicating the

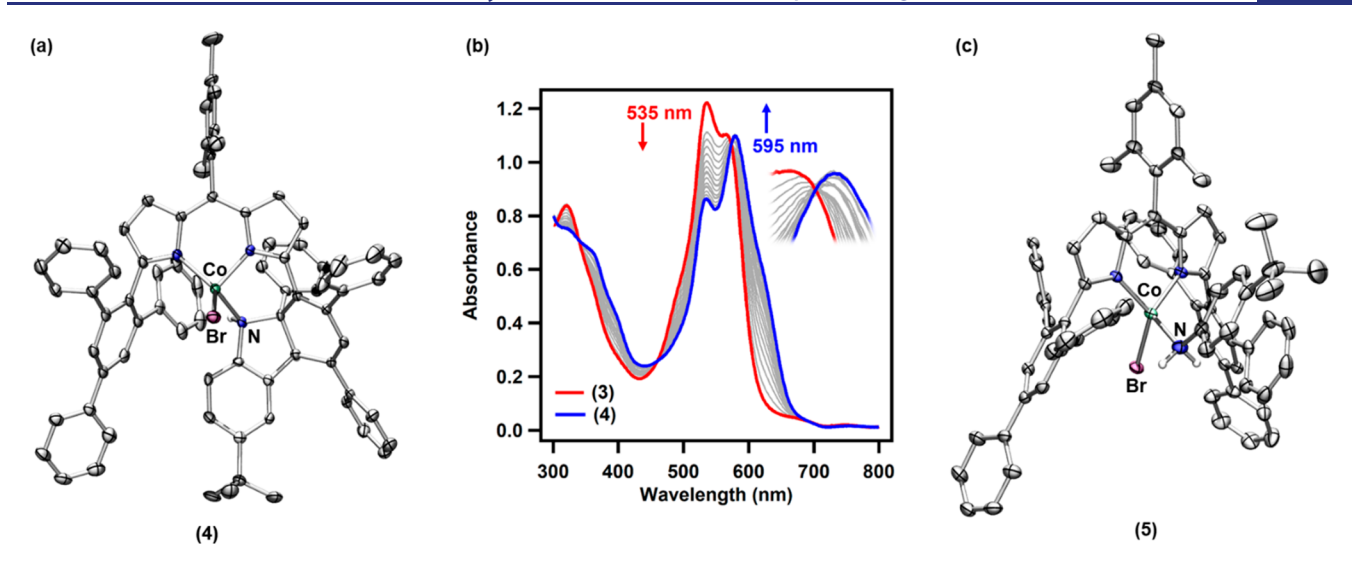


Figure 4. (a) Solid-state structure for 4 at 100 K with the thermal ellipsoids set at the 50% probability level (hydrogen atom except for N-H and solvent molecules are omitted for clarity; Co aquamarine, C gray, N blue, Br maroon, H white). (b) UV/vis traces for the conversion of 3 to 4 in benzene at 50 °C with spectra recorded every 30 min for 20 h. (c) Solid-state structure for 5 at 100 K with the thermal ellipsoids set at the 50% probability level (hydrogen atoms except for aniline N-H and solvent molecules are omitted for clarity; Co aquamarine; C gray; N blue; Br maroon; H white).

absence of π -backbonding (Figure 3a). Additionally, the frozen toluene solution EPR spectrum of 3 at 4 K displays a typical hyperfine structure of a high-spin ($S=^3/_2$) Co^{II} center, validating the redox-innocent ligation of the azide moiety (Figure 3b). These spectroscopic data are further corroborated with single-point DFT calculations using the crystallographic coordinates of 3 to illustrate that the unpaired spin density ($S=^3/_2$) is mostly localized on the cobalt center (Figure 3c). Thus, we believe that the bonding between the cobalt and the aryl azide can be best depicted as a redox-neutral, Lewis acid—base interaction. This electronic structure assignment is in accord with the previous report by Marynick which showed that in the absence of π -backbonding, coordination through N_α is favored as the substituted nitrogen atom (N_α) is more basic than the terminal N_ν .

2.3. N-Group Transfer Reactivity of 3. With a comprehensive understanding of the electronic properties of 3, we sought to investigate its N_2 extrusion reactivity and subsequent N-group transfer chemistry. While 3 is relatively stable at low temperatures, slow decay to a new paramagnetic species was observed over 3 days at room temperature. The same transformation was completed in 20 h at 50 °C accompanied by a color change from maroon to purple.

Single crystals of the purple product were grown from a hexane/benzene mixture (2:1) stored at $-35\,^{\circ}$ C. Interestingly, the solid-state structure of the species revealed a N₂-released product (4), which is formed upon ligand functionalization. The central phenyl ring of one of the 2,4,6-triphenylphenyl substituents from $^{\rm Ar}$ L is dearomatized following a [3 + 2] annulation with the parent aryl azide fragment. The aryl moiety of the parent azide restores its aromaticity upon a subsequent H—atom transfer (HAT). Additionally, the solid-state structure highlights the *syn*-addition of the nitrene moiety into the phenyl group (Scheme 2, Figure 4a).

For this unique annulation process, either a Co^{III} iminyl $(^{Ar}L)CoBr(^{\bullet}N(C_6H_4-p^{-t}Bu))$ or a Co^{IV} imido $(^{Ar}L)CoBr(N-(C_6H_4-p^{-t}Bu))$ species could serve as a potential intermediate. Given that the aryl moiety of the parent azide is engaged in the transformation, we propose that the Co^{III} iminyl complex

would be the more relevant intermediate, as significant radical delocalization throughout the aryl unit was observed for the iron analogue (^{Ar}L)FeCl($^{\bullet}N(C_6H_4-p^{-t}Bu)$). 11

The conversion from 3 to 4 exhibits no accumulation of intermediate species by ¹H NMR spectroscopy and clean isosbestic points (at $\lambda = 340$, 460, and 575 nm) are observed via UV/vis spectroscopy (Figure 4b), presumably due to a fast [3 + 2] annulation process following loss of N_2 . Nevertheless, in the presence of excess 1,4-cyclohexadiene, a benzene- d_6 solution of 3 exclusively furnished the corresponding anilinebound Co^{II} complex (ArL)CoBr(NH₂(C₆H₄-p-^tBu)) (5) at 50 °C, likely following two sequential H-atom abstraction (HAA) steps mediated by the proposed Co-nitrene intermediates (Scheme 2, Figure 4c). Furthermore, at room temperature, exposure of 3 to either 200 equiv of styrene in benzene or neat cyclohexene afforded the corresponding aziridine product (1-(4-(tert-butyl)phenyl)-2-phenylaziridine) or amination product (4-(tert-butyl)-N-(cyclohex-2-en-1-yl)aniline) in 34% and 21% yield, respectively (Scheme 2). Along with the desired products, in both cases, formation of the corresponding diazene and aniline was also detected. Similar diazene generation has been observed in several other N-group transfer reactions mediated by the corresponding metal-nitrene complexes. 13,33,35 These results corroborate the presence of a transient Co-nitrenoid equivalent and demonstrate its viability as a nitrene-group delivery reagent. 14,15,53-59

2.4. Reactivity of Dipyrrinato Co^{II} Alkyl Azide Adducts. Encouraged by the *N*-group transfer reactivity of 3, we attempted to expand the C—H amination reactivity by modifying the bound organoazide. Particularly, we were inspired by our previously reported Fe-catalyzed intramolecular C—H amination which is mediated by a high-spin ferric alkyl iminyl complex. ^{12,60} Given that we propose 3 furnishes an analogous high-valent intermediate, we envisioned that the similar transformation affording *N*-heterocyclic compounds might be feasible by replacing the aryl azide of 3 with an alkyl azide.

Akin to the synthesis of 3, we were able to prepare a series of alkyl azide-bound cobalt complexes by treating 2 with a

Scheme 3. Synthesis and Reactivity of Dipyrrinato Co^{II} Alkyl Azide Adduct Complexes

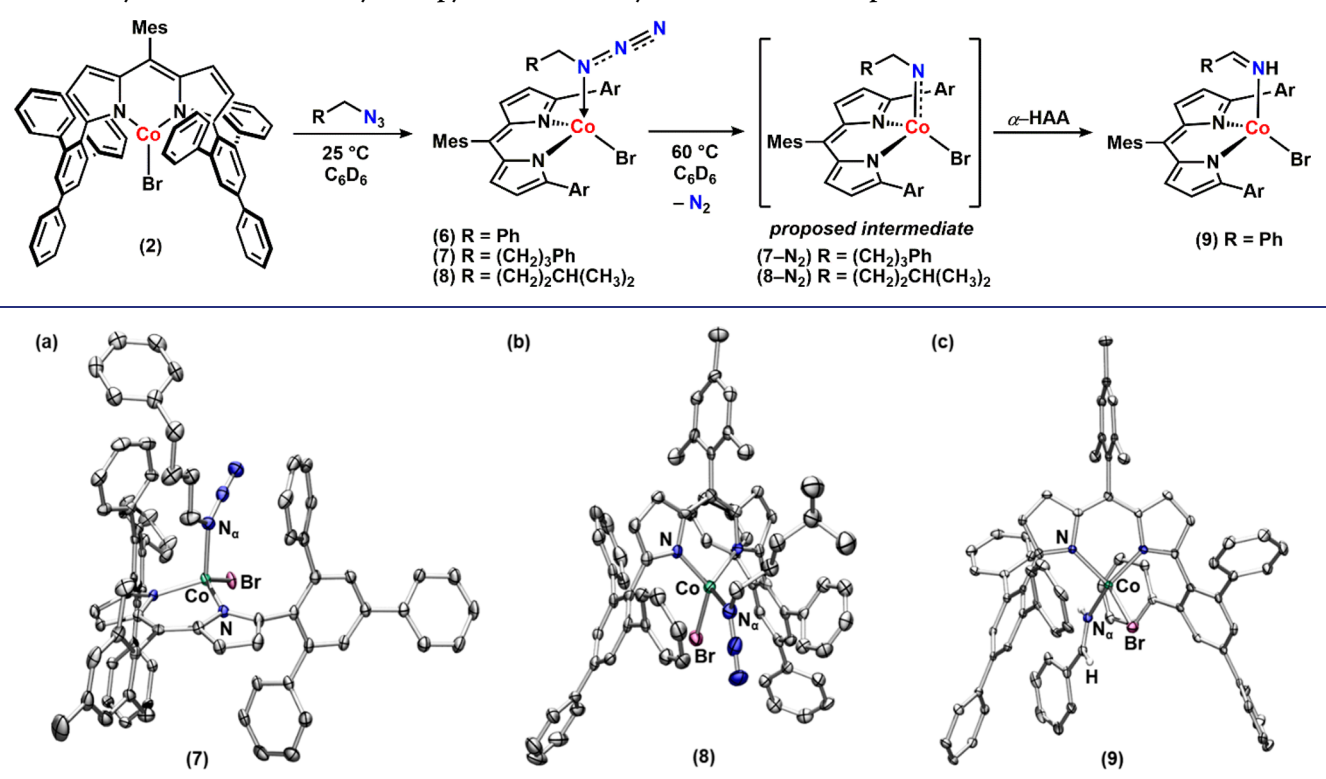


Figure 5. Solid-state structures for (a) 7, (b) 8, and (c) 9 at 100 K with thermal ellipsoids at the 50% probability level (hydrogen atoms except for imine moiety of 9 and solvent molecules are omitted for clarity; Co, aquamarine; C, gray; N, blue; Br, maroon; and H, white).

stoichiometric amount of organoazides such as benzyl azide, (4-azidobutyl)benzene, or 1-azido-4-methylpentane (Scheme 3, complexes 6, 7, and 8, respectively). α -Gem-dimethyl substituted alkyl azides, however, do not bind to 2 likely owing to the steric hindrance around the N_{α} atom, suggesting that the innate binding preference for N_{α} over N_{γ} is retained. Indeed, the solid-state structures of 7 and 8 revealed that each azide binds through the N_a with a Co- N_a distance 2.041(3) Å and 2.053(4) Å, respectively (Figure 5a and 5b). Similar to 3, both 7 and 8 exhibit a distorted trigonal monopyramidal geometry with τ_4 = 0.84 and 0.81, respectively. Additionally, solution IR spectrum of 8 displays a distinct blue-shifted azide stretch by 46 cm⁻¹ relative to the free azide (Figure S2). The frozen toluene EPR spectrum of 8 features a hyperfine structure for high-spin Co^{II}, indicating a similar dative interaction of the alkyl azide as observed for the aryl congener 3 (Figure S6). Given that adducts of linear alkyl azides are often proposed as intermediates for the transition-metal-mediated ring-closing catalysis to generate N-heterocycles, it is noteworthy that no such adduct has been structurally characterized prior to this study. 12,42,44,61

Interestingly, these alkyl azide-bound $\mathrm{Co^{II}}$ complexes display distinct kinetic profiles from 3. First, unlike 3, none of these complexes (6-8) expels $\mathrm{N_2}$ at room temperature. Instead, upon heating to 60 °C in benzene- d_6 , quantitative formation of the corresponding imine adduct was observed (Scheme 3). In the case of 6, the corresponding benzyl imine bound complex (9) was crystallographically characterized with a $\mathrm{Co-N_\alpha}$ distance of 2.029(2) Å (Figure 5c). A similar transformation has been observed in our previous studies on C–H amination catalysis mediated by either a ferric iminyl 10,12 or a cobalt imido 46 species via rapid intramolecular α -HAA. Thus, the

reactivity of 6-8 is in line with our proposed generation of a Co^{III} iminyl or Co^{IV} imido intermediate (Scheme 3). Moreover, unlike the conversion process of 3 to 4 showing no accumulation of intermediates, a paramagnetic intermediate was observed by ¹H NMR spectroscopy while heating a benzene- d_6 solution of 8 at 60 °C to afford the corresponding imine adduct (Figure S7). We speculated that the observed transient intermediate could be the proposed cobalt nitrene complex. However, our attempts to isolate the intermediate were unsuccessful due to the rapid subsequent α -HAA.

2.4.1. In Crystallo Thermal Extrusion of N_2 from **8**. We envisioned that observation of the N_2 -released intermediate (e.g., 7- N_2 and 8- N_2 in Scheme 3) may be accomplished within a crystal lattice upon thermolysis. ⁶²,63 Given that 8 reacts above 60 °C in solution, a single crystal of 8 was heated to 345 K on an X-ray diffractometer for 5–10 min followed by cooling back to 100 K for full data collection. The thermolysis was repeated four times on the same single crystal of 8 until the crystal decomposed and each data set was compared to the initial 100 K X-ray structure to monitor relative changes in occupancy of the nitrogen atoms $(N_{\alpha}, N_{\beta}, N_{\beta})$ and N_{γ}) and the bond distance between Co and the bound nitrogen atom (N_{α}) .

Indeed, noticeable changes in occupancy of the N_{β} and N_{γ} were observed while the space group of the crystal (monoclinic $P2_1/c$) did not change. Specifically, the occupancies of N_{β} and N_{γ} decreased by 16% (relative conversion) upon the first heating and by an additional 4% (relative conversion) over the subsequent three heating iterations to afford an overall 20% conversion. On the basis of the relatively subtle changes in the occupancies of nitrogen atoms over the last three heating iterations, we propose that the solid-state reaction reached maximum conversion within a few minutes. 64 Nevertheless,

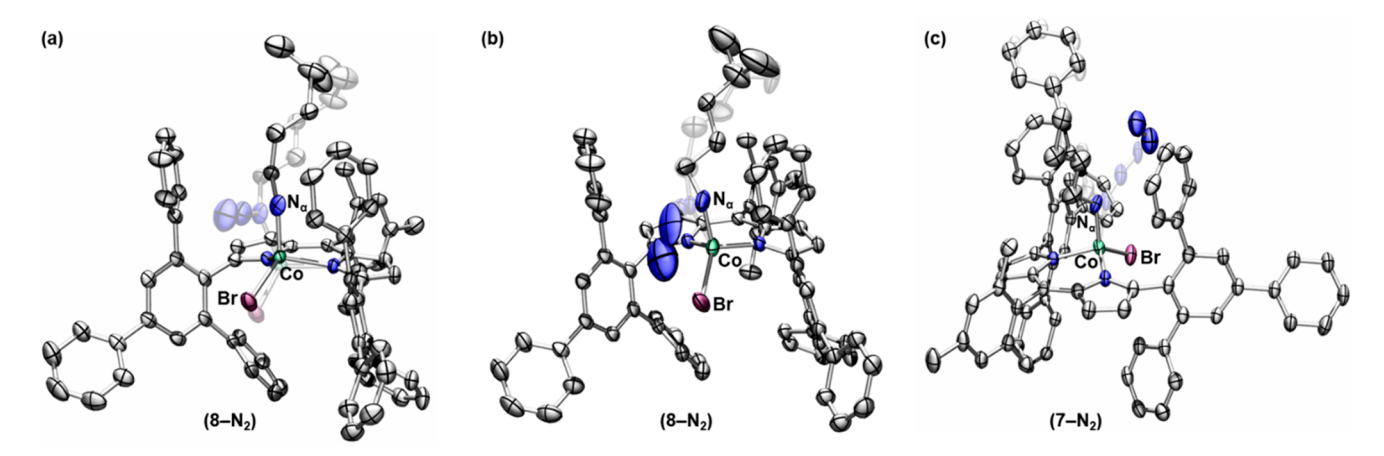


Figure 6. Solid-state structures for (a) 8-N₂ collected at 100 K following heating to 345 K, (b) 8-N₂, and (c) 7-N₂ collected at 100 K upon X-ray irradiation with thermal ellipsoids at the 50% probability level (hydrogen atoms and solvent molecules are omitted for clarity; Co, aquamarine; C, gray; N, blue; and Br, maroon).

because the quality of the single crystal sample decays upon N₂ escape from the crystal lattice, we cannot fully exclude the possibility that the lower quality of the crystal inhibits observation of higher conversions. 65,66 The results suggest that loss of N_2 occurred upon cleavage of the N_α - N_β bond as indicated in a reaction-difference map (Table S2 and Figure S26). The reaction difference map indicates the difference between the two data sets obtained before and after the four iterations of heating of the same single crystal of 8. While almost no change has been detected for the ancillary ligand (ArL), a significantly shorter Co-N_{α} distance 1.82(3) Å as compared to the initial distance of 2.053(4) Å was observed from the final model of 8-N2 which is refined based on the changes in the reaction-difference map (Figure 6a). We do not refine electron density for the extruded N2, which is likely lost from the crystal at the elevated temperatures.⁶⁷

Given that one of our previously reported four-coordinate Co^{III} complexes, a metallacycloindoline ($^{\rm Ar}L$)Co(κ^2 -NHC $_6$ H $_2$ -2,4-Me $_2$ -6-CH $_2$) exhibits a Co–N bond length of 1.845(3) Å, 45 the observed Co–N $_\alpha$ bond length (1.82(3) Å) suggests that 8-N $_2$ is likely a Co^{III} iminyl rather than a Co^{IV} imido complex. Furthermore, computational analysis on 8-N $_2$ reveals significant spin density localized on the N $_\alpha$ suggesting that the nitrenoid (NR) unit is more likely an open-shell iminyl (2 NR $^{1-}$) as opposed to a closed-shell imido (NR $^{2-}$), proposing that 8-N $_2$ can be best described as a Co^{III} iminyl rather than a Co^{IV} imido (Tables S4 and S5).

2.4.2. In Crystallo X-ray Induced N₂-Extrusion from 7 and 8. In order to gain further evidence for the proposed intermediate and minimize the heat-induced crystal decay, we have performed the similar experiments at a significantly lower temperature (100 K) upon irradiation with a high-flux Xray source. 68,69 Indeed, in crystallo N2 loss was also observed when crystallographic data were collected using a synchrotron source (0.41328 Å, 30 keV) at the Advanced Photon Source (APS), Argonne National Laboratory (ANL). Prolonged irradiation of each of 7 and 8 with a high-flux synchrotron source led to the X-ray induced conversion to 7-N₂ (69% conversion) and 8-N₂ (65% conversion), respectively. Conversion was calculated based on occupancy changes of the N_{β} and N_{γ} (Figures S28 and S29). Both 7-N₂ and 8-N₂ exhibit significantly contracted Co- N_a distances of 1.840(7) Å and 1.787(8) Å, respectively, which are in agreement with the

preliminary result observed upon thermolysis (Figure 6b,c). In contrast to the result from thermolysis and presumably due to the lower temperature at which it was generated, the extruded N_2 moiety was observed along with the proposed iminyl complex. On the basis of the observation that evolved N_2 is not observed in 8-heat (1–4) (presumably due to diffusion out of the crystalline sample), we allowed the N_2 occupancy to refine independent of the occupancy of the iminyl fragment. X-ray induced elimination of N_2 from 7 or 8 was not observed using rotating anode sources, and thus these observations indicate that N_3 activation is induced by sufficiently high-flux X-ray irradiation. Similar flux-induced chemical reactions have been observed in disulfide cleavage reactions during prolonged X-ray irradiation of protein samples and has been suggested to arise as a mechanism to dissipate absorbed X-ray energy.

These results closely parallel recent observations of photochemical and X-ray induced loss of N_2 from Ru_2 azide and Rh_2 adamantyl azide complexes, which resulted in nitride and nitrene intermediates, respectively. Combined with the present example of N_2 loss from a cobalt complex featuring organic azide ligands, this suite of reports highlights the potential of in crystallo chemical transformations to provide access to crystalline samples of reactive intermediates that are insufficiently stable to be handled by more classical methods. Further, while in the Ru_2 and Rh_2 examples, significant conversion was obtained in the solid state, the current case highlights the potential to derive chemically meaningful structural information even from incompletely converted crystalline samples.

The significantly contracted Co-N_{α} distances lead us to formulate 7-N₂ and 8-N₂ as the corresponding $\text{Co^{III}}$ -iminyl complexes. Given high errors in our X-ray studies as a result of rapid crystal decomposition during data collection and the fact that detecting the presence of H-atoms is often limited by single crystal X-ray diffraction techniques, we cannot completely exclude the possibility that the observed N₂-released structures (7-N₂ and 8-N₂) could be either the corresponding $\text{Co^{III}}$ amide (NHR) or $\text{Co^{II}}$ imine (NH=CHR') complexes. Our assignment is supported by the observation that both 7 and 8 are stable at room temperature (as indicated by ¹H NMR spectroscopy (Figures S16)) and their chemical composition has been corroborated by CHN elemental analysis, which excludes cocrystallization of 7 or 8

Scheme 4. Synthesis of 10, 11, and 12

Figure 7. (a) Solid-state structures for (a) 11, (b) 12, and (c) 14-Br at 100 K with thermal ellipsoids at the 50% probability level (hydrogen atoms and solvent molecules are omitted for clarity; Co, aquamarine; C, gray; N, blue; O, red; and Br, maroon).

Scheme 5. 1,3-Dipolar Cycloaddition Reactivity

along with their corresponding Co^{III} amide or Co^{II} imine complex. Moreover, neither 7 nor 8 exhibits intermolecular HAA reactivity as mentioned in section 2.4, suggesting that formation of a Co^{III} amide complex is highly unlikely, especially in the solid-state. Lastly, as mentioned above, $7\text{-}N_2$ and $8\text{-}N_2$ display significantly different $Co\text{-}N_\alpha$ distances with respect to the one from the authentic imine adduct 9 (2.029(2) Å). However, we emphasize that further studies and spectroscopic characterization will be necessary to better assign these compounds' identity and understand their electronic structure.

2.5. Ligand Modification for a Sterically Accessible Co^{II} Synthon. With a better understanding of the structures and reactivity of Co-organoazide adducts and the resulting Conitrene complexes, we hypothesized that the steric hindrance of ^{Ar}L limits the flexibility of the alkyl chain of 7 and 8, thus precluding the desired cyclization. As such, we attempted to synthesize a sterically more accessible dipyrrinato Co^{II} synthon. Metalation of (^{tBu}L)Li (^{tBu}L = 5-mesityl-(1,9-di-tert-butyl)dipyrrin) with anhydrous CoCl₂ or CoBr₂ in diethyl ether followed by refluxing in toluene afforded the dimeric species [(^{tBu}L)CoCl]₂ (10) and [(^{tBu}L)CoBr]₂ (11), respectively (Scheme 4, Figure 7a). Complexes 10 and 11 are

suitable synthons to explore further reactivity with organoazides as they do not feature exogenous solvent molecules which can potentially hamper the desired binding of organoazide substrates. Moreover, such dimers can readily dissociate into the corresponding solvent-bound monomeric species, when exposed to Lewis basic molecules, as exemplified by the thf-adduct 12 (Scheme 4, Figure 7b). This result suggests a similar dissociation may be possible in the presence of organoazides to generate the corresponding monomeric organoazide-bound complex.

Indeed, upon treatment of either 10 or 11 with a stoichiometric amount of 6-azidohex-1-ene, the immediate formation of the corresponding azide adduct (13) was confirmed by ^1H NMR spectroscopy (Scheme 5). Interestingly, a benzene- d_6 solution of 13 readily converts into a new paramagnetic species at room temperature, identified as the corresponding 1,2,3-dihydrotriazole-bound cobalt complex (14) via X-ray diffraction studies (Scheme 5, Figure 7c). The solid-state structure of 14-Br displays the product bound through the N $_\gamma$ instead of N $_\alpha$, presumably due to the steric encumbrance around the trisubstituted N $_\alpha$. It is noteworthy that the reaction occurs at room temperature, since in the absence of metal complexes, a similar transformation occurs

Scheme 6. Intramolecular C-H Amination or Activation

(a) C-H amination in the presence of weak C-H bonds at C₄ position

$$[(^{fBu}L)^{\textbf{CoCl}}]_{2} \\ (10) \\ \hline \\ C_{6}D_{6} \\ \hline \\ (15) \\ R^{1} = Ph, \\ R^{2} = H \\ (17) \\ R^{1} = Me, \\ R^{2} = Me \\ \hline \\ (16) \\ R^{1} = Ph, \\ R^{2} = H \\ (18) \\ R^{1} = Me, \\ R^{2} = Me \\ \hline \\ (18) \\ R^{1} = Me, \\ R^{2} = Me \\ \hline \\ (18) \\ R^{1} = Me, \\ R^{2} = Me \\ \hline$$

(b) α -H-atom abstraction in the absence of weak C-H bonds at C₄ position

$$[(^{fBu}L)^{\mathbf{CoCl}}]_{2} \qquad N_{3} \qquad Mes \qquad N_{1} \qquad \alpha - HAA \qquad \alpha - HAA \qquad Mes \qquad N_{1} \qquad C_{1} \qquad Mes \qquad N_{1} \qquad C_{2} \qquad Mes \qquad N_{1} \qquad C_{2} \qquad Mes \qquad N_{2} \qquad (19)$$

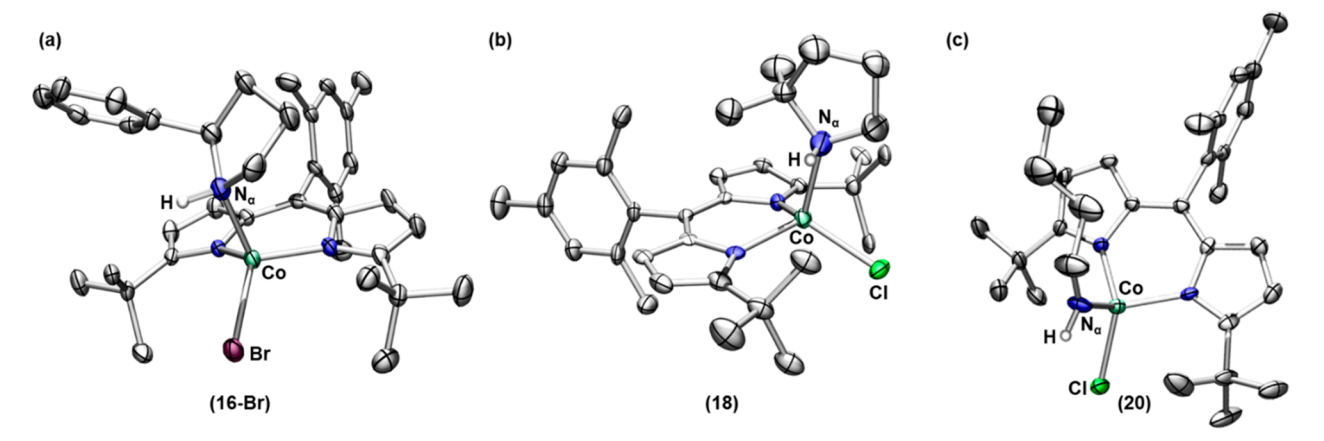


Figure 8. Solid-state structures for (a) 16-Br, (b) 18, and (c) 20 at 100 K with thermal ellipsoids at the 50% probability level (hydrogen atoms except for N-H and solvent molecules are omitted for clarity; Co, aquamarine; C, gray; N, blue; Br, maroon; Cl, green; and H, white.).

only upon refluxing with an activated olefin moiety. Furthermore, as 1,3-dipolar cycloadditions are generally facilitated by Lewis-acids, 75-78 the observation is in line with our assignment that the cobalt center is Lewis acidic. The observed cycloaddition transformation supports our initial hypothesis that smaller substituents on the dipyrrin platform enhance the flexibility of the alkyl chain.

Encouraged by this result, we next subjected a series of alkyl azides lacking internal olefins, such as (4-azidobutyl)benzene, 1-azido-4-methylpentane, or 1-azidobutane to a benzene- d_6 solution of 10. In all cases, the corresponding alkyl azidebound complexes were generated immediately at room temperature as judged by ¹H NMR spectroscopy (Scheme 6, complexes 15, 17, and 19). Akin to 2, neither 10 nor 11 binds α -gem-dimethyl substituted alkyl azides suggesting the binding propensity toward the N $_{\alpha}$ atom is maintained. Furthermore, solution IR spectra of these adducts in benzene exhibit a blueshifted azide stretch validating that the azide coordination is redox innocent (Figures S3–S5).

In contrast to 7 or 8, however, our attempts to isolate any of these azide-bound species were unsuccessful due to a greater driving force to regenerate the initial dimeric species (10 or

11) during crystallization, emphasizing the reversible binding of the organoazide. Nonetheless, the maximum value in the Job plot between 11 and 1-azido-4-methylpentane appeared at 0.5 mole fraction of a total concentration of Co^{II} center ([Co^{II}]_{total} = 2[11]) suggesting a 1:1 complexation of a single Co^{II} center and each of the organoazides to afford a monomeric species (e.g., 17) (Figure S9). Moreover, the changes in ¹H NMR chemical shifts of 11 as a function of concentration of organoazides to the corresponding monomeric organoazide adducts are almost identical regardless of the identity of the aliphatic group of the azide substrates, suggesting the nearly same binding affinities of the azides to a Co^{II} center (Figure S10).

Gratifyingly, upon heating a benzene- d_6 solution of 15 and 17 at 40 °C, we observed clean formation of the corresponding pyrrolidine-bound complexes (16) and (18), respectively (Scheme 6a, Figure 8a,b). It is notable that loss of N_2 from 15 and 17 occurs at a lower temperature compared to the reactivity observed from 7 and 8 and proceeds without any imine formation. Surprisingly, at the same temperature (40 °C), no reaction was observed for 19, which possesses a stronger, primary C–H bond at the C_4 position of the alkyl

chain. Instead, 19 expels N_2 upon heating to 80 °C to afford the corresponding imine adduct (20) via α -HAA (Scheme 6b, Figure 8c). Given that N_2 elimination is irreversible, these observations suggest the following: (1) the temperature required for N_2 expulsion and subsequent cyclization depends on the C–H bond strength on the fourth carbon (C_4) of the linear alkyl azide and (2) there is no formation of an N_2 -released intermediate (such as a Co^{IV} imido or Co^{III} iminyl species) at relatively low temperatures as the azide moiety of 19 remains intact at 40 °C.

Thus, we hypothesize that activation of the azide moiety can be induced by the interaction with C–H bonds when those bonds are weak enough to be activated, suggesting that the azide adducts themselves are viable species for C–H amination. To further support this hypothesis, we heated a benzene- d_6 solution of 19 in the presence of excess 1,4-cyclohexadiene to investigate whether an external weak C–H bond can promote loss of N_2 at a lower temperature. Indeed, under these conditions, slow conversion to the corresponding amine adduct (21) was observed at 40 °C (Scheme 7, Figure

Scheme 7. Intermolecular H-Atom Abstraction from 19

Mes
$$C_1$$
 C_2 C_3 C_4 C_5 C_6 C_6

S11). Recalling that 19 expels N_2 only above 80 $^{\circ}$ C in the absence of 1,4-cyclohexadiene, this result supports the idea that the interaction of the azide moiety with a weak C–H bond is a key step toward N_2 release and subsequent C–H amination.

Taken together, we propose two distinct pathways for activation of the azide moiety followed by intramolecular C-H amination or C-H activation. First, in the presence of

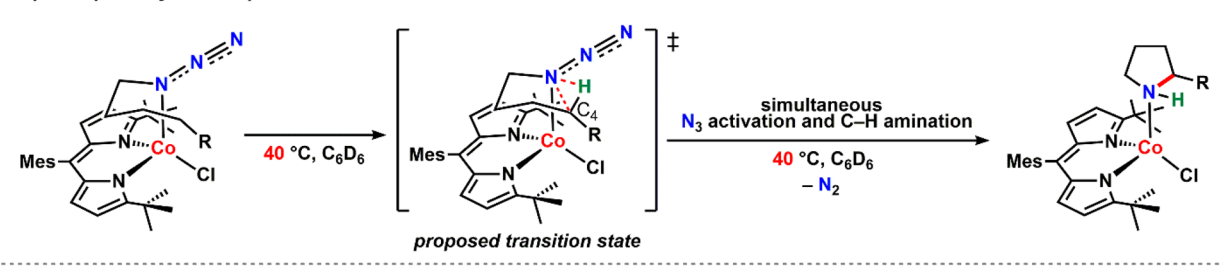
relatively weak C-H bonds (e.g., benzylic or tertiary C-H bonds), we believe that formation of pyrrolidines is directly mediated by the azide adducts, rather than a high-valent intermediate such as a Co^{IV} imido or Co^{III} iminyl species (Scheme 8, pathway I). Such direct nitrene group transfer reactivity has been previously proposed from a few metalorganoazide adduct complexes. For example, benzylic C-H bond amination and olefin aziridination catalyzed by Co³⁸ and Ru⁴⁰ porphyrin complexes, respectively, are proposed to be mediated by azide adduct species as opposed to the corresponding metal nitrene complexes. Likewise, C-H activation or group transfer reactions promoted by a simple oxidant adduct is not only limited to organoazide-bound complexes but also observed for iminoiodinane (ArI=NTs), iodosylarene (ArIO) or iodoxyarene (ArIO₂) adducts, 80,81 suggesting that metal-ligand multiply bonded species are not always the active group transfer reagents. While we cannot fully exclude the presence of a high-energy intermediate complex such as a reorganized form of the azide adducts for this specific route (pathway I), we propose that these cobalt-organoazide adducts serve as active group transfer reagents. Furthermore, we believe that a key feature enabling pathway I is the sterically accessible dipyrrin scaffold ^{tBu}L facilitates the positioning of the weak C-H bonds at C4 proximal to the azide moiety for concomitant C-H activation and C-N bond formation; whereas proximal orientation of the substrate C-H bonds is not possible for the more sterically encumbered ArL. Second, in the absence of proximal weak C-H bonds, C-H activation (i.e., α -HAA) may be mediated by the corresponding Co^{IV} imido or Co^{III} iminyl intermediates, which can be generated at relatively high temperatures via thermal N₂ extrusion (Scheme 8, pathway II). We propose that such intermediates generated at high temperatures would structurally resemble the Conitrene complexes described in Sections 2.4.1. and 2.4.2.

3. CONCLUSIONS

In this report, we demonstrated the synthesis of a series of organoazide-bound dipyrrinato Co^{II} complexes and highlighted that their nitrene group transfer reactivity can be tuned by the (1) identity of the bound organoazide (aryl azide versus alkyl

Scheme 8. Proposed Pathways for Intramolecular C-H Amination or Activation

Proposed pathway I: in the presence of weak C-H bonds



Proposed pathway II: in the absence of weak C-H bonds

azide) and (2) steric properties of the substituents on the dipyrrin scaffold (2,4,6-triphenylphenyl versus tert-butyl). First, by utilizing a sterically encumbered ligand ArL, the binding mode of the organoazides was characterized by single-crystal X-ray diffraction, solution IR spectroscopy, and EPR spectroscopy (at 4 K) to identify a redox neutral coordination through the N_{α} preferentially over N_{ν} . Although such binding mode is consistent among varying the R substituents (aryl versus alkyl) of the organoazides, we observed notably different kinetics for N₂ extrusion as well as scope of N-group transfer reactivity. For instance, the aryl azide-bound complex 3 eliminates N2 at room temperature to undergo either intra- or intermolecular C-H amination. We propose that such transformations are mediated by a Co^{IV} imido or Co^{III} iminyl species, yet no accumulation of intermediates was spectroscopically detected. In contrast, the analogous complex 8 featuring an aliphatic azide expels N₂ only above 60 °C, and an intermediate species was observed during the conversion into the corresponding imine compound. Although isolation of the intermediate was not feasible in solution due to the facile subsequent α -HAA, we were able to cleave the N-N bond within a crystal lattice to observe the corresponding N2-released structure, which we have assigned as the corresponding Co-nitrenoid (i.e., Co^{III}(²NR), Co^{IV}(NR)) complex. Future work will focus on studying the electronic structure of the Co-nitrene complexes via in-depth spectroscopic characterizations.

Lastly, by employing a more sterically accessible CoII synthon 10 or 11, intramolecular 1,3-dipolar cycloaddition as well as C-H amination to generate the 1,2,3-dihyrotriazole and substituted pyrrolidine products, respectively, were accomplished. Most importantly, our observations on reactivity patterns of alkyl azide adducts supported by the smaller dipyrrin scaffold (15, 17, and 19) suggest that organoazidebound complexes themselves are competent for the desired C-H amination when weak C-H bonds are positioned proximal to the azide moiety. This demonstrates that organoazide adducts can also be viable species for C-H amination along with the typically invoked N-group transfer reagents such as metal nitrene complexes. We believe this study provides great insight toward understanding the nature and reactivity of commonly not isolable organoazide-bound metal complexes for C-H amination processes.

ASSOCIATED CONTENT

Supporting Information

The Supporting Information is available free of charge at https://pubs.acs.org/doi/10.1021/jacs.0c04252.

General experimental considerations and procedures, multinuclear NMR data, IR spectra, EPR spectra, and computational details (PDF)

Crystallographic data (CIF)

AUTHOR INFORMATION

Corresponding Author

Theodore A. Betley — Department of Chemistry and Chemical Biology, Harvard University, Cambridge, Massachusetts 02138, United States; oorcid.org/0000-0001-5946-9629; Email: betley@chemistry.harvard.edu

Authors

Yunjung Baek — Department of Chemistry and Chemical Biology, Harvard University, Cambridge, Massachusetts 02138, United States; Ocid.org/0000-0003-3727-1077

Anuvab Das — Department of Chemistry, Texas A&M University, College Station, Texas 77843, United States; orcid.org/0000-0002-9344-4414

Shao-Liang Zheng — Department of Chemistry and Chemical Biology, Harvard University, Cambridge, Massachusetts 02138, United States; Occid.org/0000-0002-6432-9943

Joseph H. Reibenspies — Department of Chemistry, Texas A&M University, College Station, Texas 77843, United States David C. Powers — Department of Chemistry, Texas A&M University, College Station, Texas 77843, United States;

orcid.org/0000-0003-3717-2001

Complete contact information is available at: https://pubs.acs.org/10.1021/jacs.0c04252

Note:

The authors declare no competing financial interest.

ACKNOWLEDGMENTS

T.A.B. acknowledges this work was supported by a grant from the NIH (GM-115815), the Dreyfus Foundation (Teacher-Scholar Award), and Harvard University. Y.B. gratefully acknowledges a Kwanjeong Graduate Student Fellowship. D.C.P. thanks the Welch Foundation (A-1907) and the U.S. Department of Energy (DE-SC0018977) for financial support. The authors thank Yu-Sheng Chen for helpful discussion. Crystal structures of 7-N₂ and 8-N₂ in section 2.4.2 were determined at ChemMatCARS Sector 15, which is housed at the APS, which is principally supported by the NSF (Grant NSF/CHE-1346572). Use of the PILATUS3 X CdTe 1M detector is supported by the NSF (Grant NSF/DMR-1531283). Use of the APS was supported by the U.S. DOE under Contract No. DE-AC02-06CH11357.

REFERENCES

- (1) Davies, H. M. L.; Long, M. S. Recent advances in catalytic intramolecular C-H aminations. *Angew. Chem., Int. Ed.* **2005**, 44 (23), 3518–3520.
- (2) Halfen, J. Recent advances in metal-mediated carbon-nitrogen bond formation reactions: aziridination and amidation. *Curr. Org. Chem.* **2005**, *9* (7), 657–669.
- (3) Davies, H. M. L.; Manning, J. R. Catalytic C-H functionalization by metal carbenoid and nitrenoid insertion. *Nature* **2008**, *451*, 417–424.
- (4) Collet, F.; Dodd, R. H.; Dauban, P. Catalytic C-H amination: recent progress and future directions. *Chem. Commun.* **2009**, *0* (34), 5061–5074.
- (5) Zalatan, D. N.; Bois, J. D. Metal-catalyzed oxidations of C-H to C-N bonds. In C-H activation. *Topics in Current Chemistry*; Yu, J.-Q., Shi, Z., Eds.; Springer: Berlin/Heidelberg, 2009, Vol. 292; pp 347–378.
- (6) Müller, P.; Fruit, C. Enantioselective catalytic aziridinations and asymmetric nitrene insertions into C–H Bonds. *Chem. Rev.* **2003**, *103* (8), 2905–2920.
- (7) Saouma, C. T.; Peters, J. C. M≡E and M≡E complexes of iron and cobalt that emphasize three-fold symmetry (E≡O, N, NR). Coord. Chem. Rev. 2011, 255 (7), 920–937.
- (8) Mehn, M. P.; Peters, J. C. Mid- to high-valent imido and nitrido complexes of iron. *J. Inorg. Biochem.* **2006**, *100* (4), 634–643.
- (9) Zhang, L.; Deng, L. Č–H bond amination by iron-imido/nitrene species. *Chin. Sci. Bull.* **2012**, *57* (19), 2352–2360.

- (10) Hennessy, E. T.; Liu, R. Y.; Iovan, D. A.; Duncan, R. A.; Betley, T. A. Iron-mediated intermolecular *N*-group transfer chemistry with olefinic substrates. *Chem. Sci.* **2014**, *5* (4), 1526–1532.
- (11) Wilding, M. J. T.; Iovan, D. A.; Wrobel, A. T.; Lukens, J. T.; MacMillan, S. N.; Lancaster, K. M.; Betley, T. A. Direct comparison of C–H bond amination efficacy through manipulation of nitrogenvalence centered redox: imido versus iminyl. *J. Am. Chem. Soc.* **2017**, 139 (41), 14757–14766.
- (12) Hennessy, E. T.; Betley, T. A. Complex *N*-heterocycle synthesis via iron-catalyzed, direct C–H bond amination. *Science* **2013**, *340* (6132), 591–595.
- (13) Iovan, D. A.; Betley, T. A. Characterization of iron-imido species relevant for *N*-group transfer chemistry. *J. Am. Chem. Soc.* **2016**, *138* (6), 1983–1993.
- (14) Goswami, M.; Lyaskovskyy, V.; Domingos, S. R.; Buma, W. J.; Woutersen, S.; Troeppner, O.; Ivanović-Burmazović, I.; Lu, H.; Cui, X.; Zhang, X. P.; Reijerse, E. J.; DeBeer, S.; van Schooneveld, M. M.; Pfaff, F. F.; Ray, K.; de Bruin, B. Characterization of porphyrin-Co(III)-'nitrene radical' species relevant in catalytic nitrene transfer reactions. J. Am. Chem. Soc. 2015, 137 (16), 5468–5479.
- (15) Lyaskovskyy, V.; Suarez, A. I. O.; Lu, H.; Jiang, H.; Zhang, X. P.; de Bruin, B. Mechanism of cobalt(II) porphyrin-catalyzed C–H amination with organic azides: radical nature and H–atom abstraction ability of the key cobalt(III)—nitrene intermediates. *J. Am. Chem. Soc.* **2011**, *133* (31), 12264–12273.
- (16) Kuijpers, P. F.; van der Vlugt, J. I.; Schneider, S.; de Bruin, B. Nitrene radical intermediates in catalytic synthesis. *Chem. Eur. J.* **2017**, 23 (56), 13819–13829.
- (17) Li, C.; Lang, K.; Lu, H.; Hu, Y.; Cui, X.; Wojtas, L.; Zhang, X. P. Catalytic radical process for enantioselective amination of C(sp³)–H bonds. *Angew. Chem., Int. Ed.* **2018**, *57* (51), 16837–16841.
- (18) Lu, H.; Li, C.; Jiang, H.; Lizardi, C. L.; Zhang, X. P. Chemoselective amination of propargylic C(sp³)–H bonds by cobalt(II)-based metalloradical catalysis. *Angew. Chem., Int. Ed.* **2014**, 53 (27), 7028–7032.
- (19) Jiang, H.; Lang, K.; Lu, H.; Wojtas, L.; Zhang, X. P. Asymmetric radical bicyclization of allyl azidoformates via cobalt-(II)-based metalloradical catalysis. *J. Am. Chem. Soc.* **2017**, *139* (27), 9164–9167.
- (20) Conradie, J.; Ghosh, A. Electronic structure of an iron-porphyrin-nitrene complex. *Inorg. Chem.* **2010**, 49 (1), 243–248.
- (21) Corona, T.; Ribas, L.; Rovira, M.; Farquhar, E. R.; Ribas, X.; Ray, K.; Company, A. Characterization and reactivity studies of a terminal copper—nitrene species. *Angew. Chem., Int. Ed.* **2016**, *55* (45), 14005—14008.
- (22) Berry, J. F. Terminal nitrido and imido complexes of the late transition metals. *Comments Inorg. Chem.* **2009**, 30 (1–2), 28–66.
- (23) Bräse, S.; Gil, C.; Knepper, K.; Zimmermann, V. Organic azides: an exploding diversity of a unique class of compounds. *Angew. Chem., Int. Ed.* **2005**, 44 (33), 5188–5240.
- (24) Barz, M.; Herdtweck, E.; Thiel, W. R. Transition metal complexes with organoazide ligands: synthesis, structural chemistry, and reactivity. *Angew. Chem., Int. Ed.* **1998**, *37* (16), 2262–2265.
- (25) Cenini, S.; Gallo, E.; Caselli, A.; Ragaini, F.; Fantauzzi, S.; Piangiolino, C. Coordination chemistry of organic azides and amination reactions catalyzed by transition metal complexes. *Coord. Chem. Rev.* **2006**, 250 (11), 1234–1253.
- (26) Proulx, G.; Bergman, R. G. Synthesis and structure of a terminal metal azide complex: an isolated intermediate in the formation of imidometal complexes from organic azides. *J. Am. Chem. Soc.* **1995**, 117 (23), 6382–6383.
- (27) Proulx, G.; Bergman, R. G. Synthesis, structures, and kinetics and mechanism of decomposition of terminal metal azide complexes: isolated intermediates in the formation of imidometal complexes from organic azides. *Organometallics* **1996**, *15* (2), 684–692.
- (28) Fickes, M. G.; Davis, W. M.; Cummins, C. C. Isolation and structural characterization of the terminal mesityl azide complex $V(N_3Mes)(I)(NRAr_F)_2$ and its conversion to a vanadium(V) imido complex. *J. Am. Chem. Soc.* **1995**, *117* (23), 6384–6385.

- (29) Harman, W. H.; Lichterman, M. F.; Piro, N. A.; Chang, C. J. Well-defined vanadium organoazide complexes and their conversion to terminal vanadium imides: structural snapshots and evidence for a nitrene capture mechanism. *Inorg. Chem.* **2012**, *51* (18), 10037–10042
- (30) Guillemot, G.; Solari, E.; Floriani, C.; Rizzoli, C. Nitrogen-to-metal multiple bond functionalities: the reaction of calix[4]arene—W(IV) with azides and diazoalkanes. *Organometallics* **2001**, 20 (4), 607–615.
- (31) Albertin, G.; Antoniutti, S.; Baldan, D.; Castro, J.; García-Fontán, S. Preparation of benzyl azide complexes of iridium(III). *Inorg. Chem.* **2008**, *47* (2), 742–748.
- (32) Dias, H. V. R.; Polach, S. A.; Goh, S.-K.; Archibong, E. F.; Marynick, D. S. Copper and silver complexes containing organic azide ligands: syntheses, structures, and theoretical investigation of $[HB(3,5-(CF_3)_2Pz)_3]CuNNN(1-Ad)$ and $[HB(3,5-(CF_3)_2Pz)_3]AgN-(1-Ad)NN$ (where Pz = Pyrazolyl and 1-Ad = 1-Adamantyl). *Inorg. Chem.* **2000**, 39 (17), 3894–3901.
- (33) Takaoka, A.; Moret, M.-E.; Peters, J. C. A Ru(I) metalloradical that catalyzes nitrene coupling to azoarenes from arylazides. *J. Am. Chem. Soc.* **2012**, *134* (15), 6695–6706.
- (34) Grant, L. N.; Carroll, M. E.; Carroll, P. J.; Mindiola, D. J. An unusual cobalt azide adduct that produces a nitrene species for carbon-hydrogen insertion chemistry. *Inorg. Chem.* **2016**, *55* (16), 7997–8002.
- (35) Mankad, N. P.; Müller, P.; Peters, J. C. Catalytic N—N coupling of aryl azides to yield azoarenes via trigonal bipyramid iron—nitrene intermediates. *J. Am. Chem. Soc.* **2010**, *132* (12), 4083—4085.
- (36) Waterman, R.; Hillhouse, G. L. η^2 -Organoazide complexes of nickel and their conversion to terminal imido complexes via dinitrogen extrusion. *J. Am. Chem. Soc.* **2008**, *130* (38), 12628–12629.
- (37) Hanna, T. A.; Baranger, A. M.; Bergman, R. G. Addition of organic 1,3-dipolar compounds across a heterobinuclear bond between early and late transition metals: mechanism of nitrogen loss from an organoazido complex to form a bridging imido complex. *Angew. Chem., Int. Ed. Engl.* **1996**, 35 (6), 653–655.
- (38) Ragaini, F.; Penoni, A.; Gallo, E.; Tollari, S.; Li Gotti, C.; Lapadula, M.; Mangioni, E.; Cenini, S. Amination of benzylic C–H bonds by arylazides catalyzed by Co^{II}–porphyrin complexes: a synthetic and mechanistic study. *Chem. Eur. J.* **2003**, 9 (1), 249–259.
- (39) Fantauzzi, S.; Gallo, E.; Caselli, A.; Ragaini, F.; Macchi, P.; Casati, N.; Cenini, S. Origin of the deactivation in styrene aziridination by aryl azides, catalyzed by ruthenium porphyrin complexes. Structural characterization of a Δ^2 -1,2,3-triazoline Ru^{II}(TPP)CO complex. *Organometallics* **2005**, 24 (20), 4710–4713.
- (40) Fantauzzi, S.; Gallo, E.; Caselli, A.; Piangiolino, C.; Ragaini, F.; Cenini, S. The (porphyrin)ruthenium-catalyzed aziridination of olefins using aryl azides as nitrogen sources. *Eur. J. Org. Chem.* **2007**, 2007 (36), 6053–6059.
- (41) King, E. R.; Hennessy, E. T.; Betley, T. A. Catalytic C–H bond amination from high-spin iron imido complexes. *J. Am. Chem. Soc.* **2011**, *1*33 (13), 4917–4923.
- (42) Shing, K.-P.; Liu, Y.; Cao, B.; Chang, X.-Y.; You, T.; Che, C.-M. N-Heterocyclic carbene iron(III) porphyrin-catalyzed intramolecular C(sp³)—H amination of alkyl azides. *Angew. Chem., Int. Ed.* **2018**, *57* (37), 11947—11951.
- (43) Goswami, M.; Geuijen, P.; Reek, J. N. H.; de Bruin, B. Application of [Co(corrole)]⁻ complexes in ring-closing C–H amination of aliphatic azides via nitrene radical intermediates. *Eur. J. Inorg. Chem.* **2018**, 2018 (5), 617–626.
- (44) Bagh, B.; Broere, D. L. J.; Sinha, V.; Kuijpers, P. F.; van Leest, N. P.; de Bruin, B.; Demeshko, S.; Siegler, M. A.; van der Vlugt, J. I. Catalytic synthesis of *N*-heterocycles via direct C(sp³)—H amination using an air-stable iron(III) species with a redox-active ligand. *J. Am. Chem. Soc.* **2017**, *139* (14), 5117–5124.
- (45) King, E. R.; Sazama, G. T.; Betley, T. A. Co(III) imidos exhibiting spin crossover and C–H bond activation. *J. Am. Chem. Soc.* **2012**, *134* (43), 17858–17861.

- (46) Baek, Y.; Betley, T. A. Catalytic C-H amination mediated by dipyrrin cobalt imidos. J. Am. Chem. Soc. 2019, 141 (19), 7797-7806.
- (47) Yang, L.; Powell, D. R.; Houser, R. P. Structural variation in copper(I) complexes with pyridylmethylamide ligands: structural analysis with a new four-coordinate geometry index, τ_4 . Dalton Trans. **2007**, *9*, 955–964.
- (48) Johnson, E. R.; Keinan, S.; Mori-Sánchez, P.; Contreras-García, J.; Cohen, A. J.; Yang, W. Revealing noncovalent interactions. *J. Am. Chem. Soc.* **2010**, *132* (18), *6498*–*6506*.
- (49) Contreras-García, J.; Johnson, E. R.; Keinan, S.; Chaudret, R.; Piquemal, J.-P.; Beratan, D. N.; Yang, W. NCIPLOT: A program for plotting noncovalent interaction regions. *J. Chem. Theory Comput.* **2011**, *7* (3), 625–632.
- (50) Neese, F. ORCA—An Ab Initio, Density Functional and Semiempirical Electronic Structure Package, version 2.9–00; Universitat Bonn: Bonn, Germany, 2009.
- (51) Das, A.; Chen, Y.-S.; Reibenspies, J. H.; Powers, D. C. Characterization of a reactive Rh₂ nitrenoid by crystalline matrix isolation. *J. Am. Chem. Soc.* **2019**, *141*, 16232–16236.
- (52) Dash, C.; Yousufuddin, M.; Cundari, T. R.; Dias, H. V. R. Gold-mediated expulsion of dinitrogen from organic azides. *J. Am. Chem. Soc.* **2013**, *135*, 15479–15488.
- (53) Jin, L.-M.; Lu, H.; Cui, Y.; Lizardi, C. L.; Arzua, T. N.; Wojtas, L.; Cui, X.; Zhang, X. P. Selective radical amination of aldehydic C(sp²)—H bonds with fluoroaryl azides via Co(II)-based metalloradical catalysis: synthesis of *N*-fluoroaryl amides from aldehydes under neutral and nonoxidative conditions. *Chem. Sci.* **2014**, 5 (6), 2422–2427.
- (54) Olivos Suarez, A. I.; Jiang, H.; Zhang, X. P.; de Bruin, B. The radical mechanism of cobalt(II) porphyrin-catalyzed olefin aziridination and the importance of cooperative H-bonding. *Dalton Trans.* **2011**, 40 (21), 5697–5705.
- (55) Subbarayan, V.; Jin, L.-M.; Cui, X.; Zhang, X. P. Room temperature activation of aryloxysulfonyl azides by [Co(II)(TPP)] for selective radical aziridination of alkenes via metalloradical catalysis. *Tetrahedron Lett.* **2015**, *56* (23), 3431–3434.
- (56) Tao, J.; Jin, L.-M.; Zhang, X. P. Synthesis of chiral *N*-phosphoryl aziridines through enantioselective aziridination of alkenes with phosphoryl azide via Co(II)-based metalloradical catalysis. *Beilstein J. Org. Chem.* **2014**, *10*, 1282–1289.
- (57) Gao, G.-Y.; Jones, J. E.; Vyas, R.; Harden, J. D.; Zhang, X. P. Cobalt-catalyzed aziridination with diphenylphosphoryl azide (DPPA): direct synthesis of *N*-phosphorus-substituted aziridines from Alkenes. *J. Org. Chem.* **2006**, *71* (17), 6655–6658.
- (58) Harden, J. D.; Ruppel, J. V.; Gao, G.-Y.; Zhang, X. P. Cobalt-catalyzed intermolecular C–H amination with bromamine-T as nitrene source. *Chem. Commun.* **2007**, *44*, 4644–4646.
- (59) Aguila, M. J. B.; Badiei, Y. M.; Warren, T. H. Mechanistic insights into C-H amination via dicopper nitrenes. *J. Am. Chem. Soc.* **2013**, 135 (25), 9399–9406.
- (60) Iovan, D. A.; Wilding, M. J. T.; Baek, Y.; Hennessy, E. T.; Betley, T. A. Diastereoselective C-H bond amination for disubstituted pyrrolidines. *Angew. Chem., Int. Ed.* **2017**, *56* (49), 15599–15602.
- (61) Broere, D. L. J.; de Bruin, B.; Reek, J. N. H.; Lutz, M.; Dechert, S.; van der Vlugt, J. I. Intramolecular redox-active ligand-to-substrate single-electron transfer: radical reactivity with a palladium(II) complex. J. Am. Chem. Soc. 2014, 136 (33), 11574–11577.
- (62) Powers, D. C.; Anderson, B. L.; Hwang, S. J.; Powers, T. M.; Pérez, L. M.; Hall, M. B.; Zheng, S.-L.; Chen, Y.-S.; Nocera, D. G. Photocrystallographic observation of halide-bridged intermediates in halogen photoeliminations. *J. Am. Chem. Soc.* **2014**, *136* (43), 15346–15355.
- (63) Das, A.; Reibenspies, J. H.; Chen, Y.-S.; Powers, D. C. Direct characterization of a reactive lattice-confined Ru₂ nitride by photocrystallography. *J. Am. Chem. Soc.* **2017**, 139 (8), 2912–2915.
- (64) Zheng, S.-L.; Pham, O.; Vande Velde, C. M. L.; Gembicky, M.; Coppens, P. Competitive isomerization and dimerization in cocrystals of 1,1,6,6-tetraphenyl-2,4-hexadiyne-1,6-diol and sorbic acid:

- a new look at stereochemical requirements for [2 + 2] dimerization. *Chem. Commun.* **2008**, 22, 2538.
- (65) Zheng, S.-L.; Wang, Y.; Yu, Z.; Lin, Q.; Coppens, P. Direct observation of a photoinduced nonstabilized nitrile imine structure in the solid state. *J. Am. Chem. Soc.* **2009**, *131* (50), 18036–18037.
- (66) Abdelmoty, I.; Buchholz, V.; Di, L.; Guo, C.; Kowitz, K.; Enkelmann, V.; Wegner, G.; Foxman, B. M. Polymorphism of cinnamic and α -truxillic acids: new additions to an old story. *Cryst. Growth Des.* **2005**, 5 (6), 2210–2217.
- (67) More specifically, for the reactive fragment, all non-H atoms of the product were located in the reaction-difference maps, calculated with coefficients $F_o(\text{heat}) F_o(\text{initial})$, and then refined with restraints on the reacted fragment's bond lengths and constraints of the atomic displacement parameters to the corresponding values of the unreacted fragment. If necessary, the restraints of the atomic displacement parameters have been applied for such disorder refinement. For the nonreactive fragment, the restraints on bond lengths, as well as the restraints of the atomic displacement parameters, have been applied for the disorder refinement as necessary. In order to get a reasonable bond length for the severely disordered hexane and avoid a nonpositive definite of atomic displacement parameters, the restraints of DFIX and ISOR were applied.
- (68) Das, A.; Van Trieste, G. P.; Powers, D. C. Crystallography of reactive intermediates. *Comments Inorg. Chem.* **2020**, *40*, 116–158.
- (69) Ohashi, Y.; Sasada, Y. X-ray analysis of Co-C bond cleavage in the crystalline state. *Nature* **1977**, *267* (5607), 142–144.
- (70) Garman, E. Radiation damage in macromolecular crystallography: what is it and why should we care? *Acta Crystallogr., Sect. D: Biol. Crystallogr.* **2010**, *66* (4), 339–351.
- (71) In the refinement of $7\text{-}N_2$ and $8\text{-}N_2$, we utilized restraints on both the unconverted starting material components of the crystals and on the N_2 that is eliminated. This strategy is required because conversion of azide to iminyl radical and N_2 generates crystalline samples in which the starting materials and products are effectively compositionally disordered (see Figures S30 and S31 for raw electron density maps). In order to derive chemically meaningful data from these electron density maps, the employed restraints are critical.
- (72) Christensen, J.; Horton, P. N.; Bury, C. S.; Dickerson, J. L.; Taberman, H.; Garman, E. F.; Coles, S. J. Radiation damage in small-molecule crystallography: fact not fiction. *IUCrJ* **2019**, *6*, 703–713.
- (73) Das, A.; Maher, A. G.; Telser, J.; Powers, D. C. Observation of a photogenerated Rh₂ nitrenoid intermediate in C–H amination. *J. Am. Chem. Soc.* **2018**, *140*, 10412–10415.
- (74) Molander, G. A.; Bibeau, C. T. Thermal rearrangements of α -(ω -azidoalkyl) enones. *Tetrahedron Lett.* **2002**, 43 (31), 5385–5388.
- (75) Suga, H.; Ebiura, Y.; Fukushima, K.; Kakehi, A.; Baba, T. Efficient catalytic effects of Lewis acids in the 1,3-dipolar cycloaddition reactions of carbonyl ylides with imines. *J. Org. Chem.* **2005**, 70 (26), 10782–10791.
- (76) Huisgen, R. Kinetics and mechanism of 1,3-dipolar cyclo-additions. *Angew. Chem., Int. Ed. Engl.* 1963, 2 (11), 633–645.
- (77) Firestone, R. A. Mechanism of 1,3-dipolar cycloadditions. *J. Org. Chem.* **1968**, 33 (6), 2285–2290.
- (78) Merino, P.; Tejero, T.; Laguna, M.; Cerrada, E.; Moreno, A.; Lopez, J. A. An investigation of the Lewis acid mediated 1,3-dipolar cycloaddition between *N*-benzyl-*C*-(2-pyridyl)nitrone and allylic alcohol. Direct entry to isoxazolidinyl *C*-nucleosides. *Org. Biomol. Chem.* **2003**, *1* (13), 2336–2342.
- (79) Zdilla, M. J.; Abu-Omar, M. M. Mechanism of catalytic aziridination with manganese corrole: the often postulated high-valent Mn(V) imido is not the group transfer reagent. *J. Am. Chem. Soc.* **2006**, *128* (51), 16971–16979.
- (80) Hill, E. A.; Kelty, M. L.; Filatov, A. S.; Anderson, J. S. Isolable iodosylarene and iodoxyarene adducts of Co and their O-atom transfer and C–H activation reactivity. *Chem. Sci.* **2018**, 9 (19), 4493–4499.
- (81) Jeong, D.; Ohta, T.; Cho, J. Structure and reactivity of a mononuclear nonheme manganese(III)—iodosylarene complex. *J. Am. Chem. Soc.* **2018**, *140* (47), 16037—16041.